

# Particle Production in 3.7A GeV $^{16}\text{O}$ Nucleus Interactions

A. Abdelsalam<sup>1</sup>, M. S. El-Nagdy<sup>2</sup>, B. M. Badawy<sup>3</sup>, W. Osman<sup>1</sup>, M. M. Mohammed<sup>1</sup>, A. Saber<sup>4</sup>,  
and M.M. Ahmed<sup>2</sup>

<sup>1</sup>Physics Department, Faculty of Science, Cairo University, Giza, Egypt.

<sup>2</sup>Physics Department, Faculty of Science, Helwan University, Cairo, Egypt.

<sup>3</sup>Reactor Physics Department, Nuclear Research Center, Atomic Energy Authority, Egypt.

<sup>4</sup>Mathematics and Physics Engineering Department, Faculty of Engineering Shoubra, Banha University, Cairo, Egypt.

\*Mohammad El-Nadi High Energy Lab, Faculty of Science, Cairo University, Egypt.

<sup>1</sup>Email: [he\\_cairo@yahoo.com](mailto:he_cairo@yahoo.com)

## ABSTRACT

Experimental study on 3.7A GeV  $^{16}\text{O}$  interactions with emulsion nuclei is carried out. The shower particle multiplicity characteristics are investigated. Data are presented in terms of the number of emitted particles in both forward and backward angular zones. The dependence on the target size is presented. For this purpose the statistical events are discriminated into groups according to the interactions with H, CNO, Em, and AgBr target nuclei. The separation of events, into the mentioned groups, is executed basing on Glauber's approach. Features suggestive of a decay mechanism seem to be a characteristic of the backward emission. This emission may be during the de-excitation of the excited target nucleus, in a behavior like that of compound-nucleus disintegration. Regarding the limiting fragmentation hypothesis beyond 1A GeV, the target size is the main parameter affecting the backward production. The incident energy is a main factor responsible for the forward emitted particle production in a creation system. However, the target size is an effective parameter as well as the projectile size considering the geometrical concept regarded in the nuclear fireball model. The data are simulated in the framework of the Lund Monte Carlo simulation code, the so-called modified FRITIOF model. The multisource thermal model can predict source numbers, may be responsible for particle production.

**Key Words:**  $^{16}\text{O}$  Interactions at Dubna Energy/ Pion Sources/ Target Size and Centrality Dependences/ Modified FRITIOF Model/ Multi Source Thermal Model.

**PACS:** 25.75.-q, 25.75.Dw, 25.75.Gz, 25.75.Ld, 25.70.Mn, 25.70.Pq, 41.75.Ak, 41.75.Cn, 29.40.Rg, 07.68.+m

## INTRODUCTION

Actually, the synchrotron accelerator at Dubna enables equipping beams of  $A \geq 1$ , in a few A GeV range of energies. This region is a special energy, at which the nuclear limiting fragmentation applies initially [1–7]. The nuclear emulsion is a very useful tool in experimental physics for investigating atomic and nuclear processes. It can be used as a detector of  $4\pi$  space geometry. Moreover, it has a wide range of target mass numbers. In this work 3.7A GeV  $^{16}\text{O}$  interactions with emulsion nuclei are used. The shower particles are mainly identified in nuclear emulsion as pions. Hence, the pion multiplicity characteristics are investigated according to the emission angular zone, target size, and centrality. The inelastic interaction samples of 3.7A GeV  $^{16}\text{O}$  in nuclear emulsion are separated into statistical groups according to the target sizes. Applying the predicted percentages of the Glauber's approach [8], we categorize the data according to the interactions with H, CNO, Em, and AgBr targets separately. The effective mass number of each target group of nuclei is 1, 14, 70, and 94,

respectively. The modified FRITIOF model, MFM, code is used to simulate the present data. It is based on the Lund version 1.6 [9, 10]. The modification was carried out by V. V. Uzhinskii, LIT, JINR, Dubna, Russia, in 1995. The predictions of the MFM are presented in the figures by histograms. The data are approximated in the framework of the multisource thermal model, MSTM [11–12]. The approximated distributions are presented in the figures by the smooth dashed curves. The characteristics of these curves are obtained as fit parameters.

## EXPERIMENTAL DETAILS

The NIKFI–BR2 nuclear emulsion stack used this experiment is irradiated by  $^{16}\text{O}$  beams at the Synchrophasotron of JINR in Dubna, Russia. The beams energy is 3.7A GeV. Each emulsion pellicle size is 20 cm  $\times$  10 cm  $\times$  0.06 cm. Table (1) shows the chemical composition of this emulsion type.

**Table (1): Chemical composition of NIKFI–BR2 emulsion.**

Element	$^1\text{H}$	$^{12}\text{C}$	$^{14}\text{N}$	$^{16}\text{O}$	$^{80}\text{Br}$	$^{108}\text{Ag}$
Atoms / $\text{cm}^3 \times 10^{22}$	3.150	1.410	0.395	0.956	1.028	1.028

The obeyed methods, equipment, and experimental restrictions are as similar as detailed in experiments [14, 15]. The produced particles are identified in photographic nuclear emulsion, according to the commonly accepted ionization behavior [16, 17], as:

- Shower particles having  $g \leq 1.4g_p$  where  $g$  is the track grain density and  $g_p$  corresponds to the grain density of the minimum ionizing track. These particles are relativistic hadrons, which consist mainly of pions and less than 10% mesons and baryons. Their multiplicity is denoted as  $n_s$ . The notations  $n_s^f$  and  $n_s^b$  correspond to the shower particles emitted in the forward hemisphere, FHS, within  $\theta_{\text{lab}} < 90^\circ$  and in the backward hemisphere, BHS, within  $\theta_{\text{lab}} < 90^\circ$  within  $\theta_{\text{lab}} < 90^\circ$ , respectively.
- Grey particles having a range  $> 3$  mm and  $1.4g_p < g \leq 4.5g_p$ ; they are mainly recoil protons knocked-out from the target nucleus during the collision. Their kinetic energy ranges from 26 up to 400 MeV.
- Black particles having a range  $\leq 3$  mm and  $g > 4.5g_p$ ; they are evaporated target protons with kinetic energy  $< 26$  MeV.
- The grey and black particles together amount the group of the target fragments, the so called heavily ionizing particles. These fragments are emitted in the  $4\pi$  space. Their multiplicity is denoted as  $N_h$ .
- The projectile fragments having  $Z \geq 1$ ; they are fragmented nuclei having nearly the same momentum of the incident nucleus. They are emitted in a very narrow forward cone along the direction of incidence.

## RESULTS and DISCUSSION

### Interaction Cross–Section

Since the nuclear emulsion is a homogeneous mixture of different nuclei, the inelastic interactions can be classified into groups according to the target nucleus. In this experiment the events discrimination depends on the theoretical predictions of the Glauber's approach [8]. The present 3.7A GeV  $^{16}\text{O}$  inelastic interaction cross section is compared with those due to 60A GeV  $^{16}\text{O}$  interacting in FUJI emulsion [18] and with EMU01 collaboration data [19]. The run Glauber's approach code [8] simulates the data which are presented by the histograms in Fig. (1).

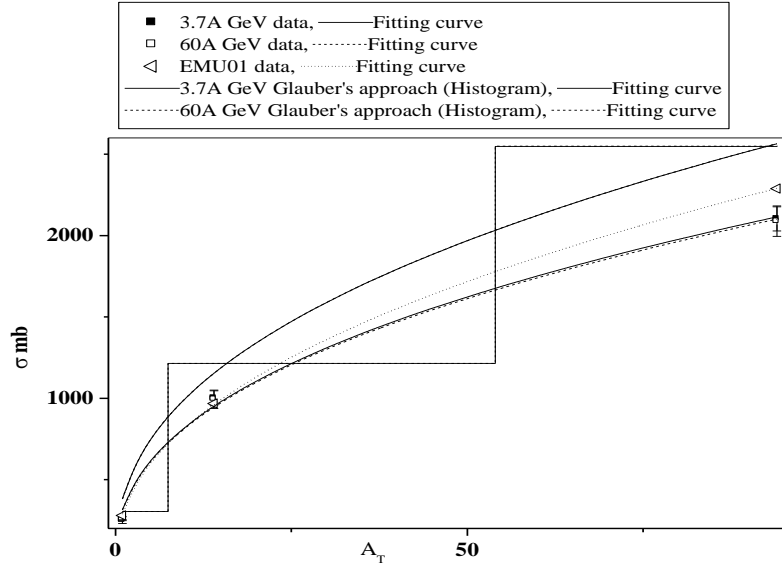


**Fig. (1): Cross section of  $^{16}\text{O}$  inelastic interactions in nuclear emulsion as a function of the target size.**

From the figure, the cross sectional values are nearly the same at the two energies. The Glauber's approach can predict them. The data are approximated by the power law relation of Eq. (1) which is presented by the smooth curves in Fig. (1). The fit parameters,  $a$  and  $b$ , are listed in Table (2). The fit parameters corresponding to the Glauber's simulations are placed in round brackets. The power is the same within experimental errors, irrespective of the energy. On average,  $a = 336$  and  $b = 0.43$ . Therefore, Eq. (1) can be rewritten as Eq. (2) which is independent on the energy.

$$\sigma = aA_T^b \quad (1)$$

$$\sigma = 336A_T^{0.43} \text{ mb} \quad (2)$$

**Table (2): Fit Parameters of Eq. (1).**

Fit Parameter	$a$	$B$
$E_{\text{lab}} = 3.7\text{A GeV}$	$314.50 \pm 51.56$ ( $381.85 \pm 62.73$ )	$0.42 \pm 0.04$ ( $0.42 \pm 0.04$ )
$E_{\text{lab}} = 60\text{A GeV}$	$312.50 \pm 50.20$ ( $381.80 \pm 62.68$ )	$0.42 \pm 0.04$ ( $0.42 \pm 0.04$ )
EMU01	$288.75 \pm 6.45$	$0.46 \pm 0.01$

### Backward Emitted Pion Multiplicity Characteristics

The backward emitted shower particle multiplicity distributions of 3.7A GeV  $^{16}\text{O}$  interactions with emulsion nuclei at average impact parameters are shown in Fig. (2).

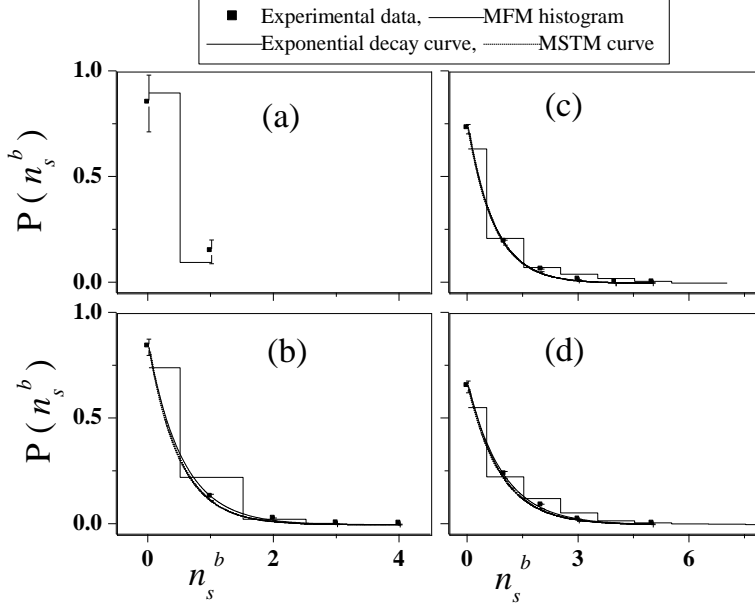


**Fig. (2): Multiplicity distributions of the backward shower particle emitted in 3.7A GeV  $^{16}\text{O}$  interactions with H, CNO, Em, and AgBr nuclei.**

From Fig. (2), the characteristic feature of the distribution is the exponential decay shape, irrespective of the target. The multiplicity range (decay tail) exceeds with the target size. The characteristic exponential behavior can be approximated by Eq. (3). The fit parameters,  $p_s^b$  and  $\lambda_s^b$ , are listed in Table (3). The data are reproduced well by the MFM. The MSTM approximated curves are superimposed on the exponential decay ones. From Table (3), the average multiplicity,  $\langle n_s^b \rangle_{\text{Exp}}$ , increases with the target size. The predicted average multiplicity,  $\langle n_s^b \rangle_{\text{MFM}}$ , overestimates the experimental one. The overestimation increases with the target size. In the framework of the MSTM the source no,  $m_1$ , is always unity. This implies that a single source is responsible for this particle production system. Hence, the decay shaped curve feature is suggested to indicate a single source production system. The weight factor of the source,  $k_1$ , increases with the target size. The resulted average multiplicities from the MSTM agree completely with the experimental data.

$$P(n_s^b) = p_s^b e^{-\lambda_s^b n_s^b} \quad (3)$$

**Table (3): Characteristic parameters associated with the backward emitted shower particle multiplicity in 3.7A GeV  $^{16}\text{O}$  interactions with emulsion nuclei at average impact parameters.**

Target	H	CNO	Em	AgBr
$p_s^b$	—	0.84	$0.74 \pm 0.02$	$0.66 \pm 0.03$
$\lambda_s^b$	—	$1.86 \pm 0.02$	$1.39 \pm 0.04$	$1.07 \pm 0.04$
j = 1	$k_1$	—	0.52	0.57
	$m_1$	—	1	1
	$\langle n_{i1} \rangle$	—	0.49	0.72
$\langle n_s^b \rangle_{\text{MSTM}}$	—	0.20	0.37	0.50
$\langle n_s^b \rangle_{\text{Exp}}$	$0.15 \pm 0.05$	$0.20 \pm 0.02$	$0.37 \pm 0.02$	$0.49 \pm 0.03$

$\langle n_s^b \rangle_{\text{MFM}}$	0.10	0.30	0.64	0.83
--------------------------------------	------	------	------	------

The backward emitted shower particle multiplicity distribution can be determined as a function of the effective target mass number,  $A_T$ , in Fig. (3). The fit parameters are approximated linearly with the target size. The slopes of the lines are  $-0.009$  and  $-0.002$  in insets a and b, respectively. In the same respect the intercepts are  $2.00 \pm 0.04$  and  $0.88 \pm 0.02$ .

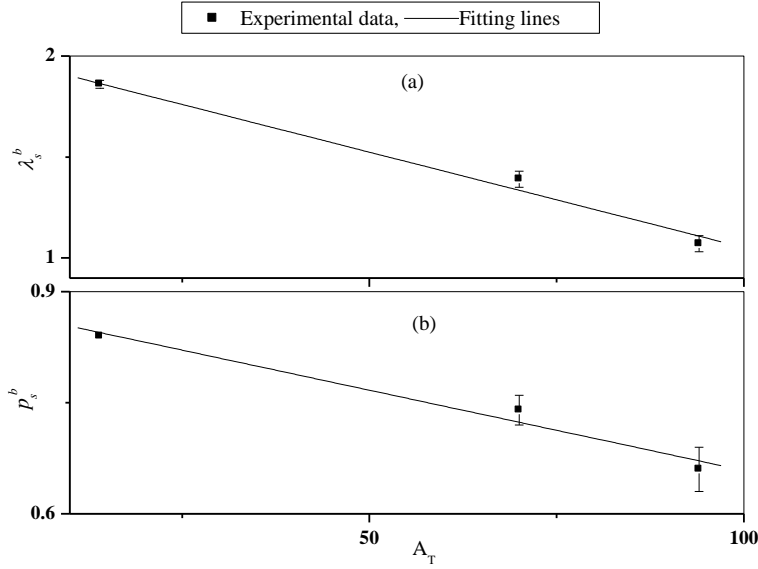


**Fig. (3):** Fit parameters of Eq. (3) as a function of the target mass number.

Independently on the projectile size ( $A_{\text{Proj}} = 1$  to  $32$ ) or energy ( $E_{\text{lab}} = 2.1A$  to  $200A$  GeV), the backward relativistic hadron is produced with probability values of  $\sim 20$  to  $30\%$  for interactions with Em target [20]. The values of  $\langle n_s^b \rangle$  are found to increase with the projectile size for  $A_{\text{Proj}} < 6$ . At  $A_{\text{Proj}} \geq 6$ , they begin to saturate and have a constant value of  $\langle n_s^b \rangle \sim 0.4$  [20]. The results show also that the energy is not an effective parameter in this backward production [20]. Therefore, one can conclude that the backward emitted pion does not come from the fireball nuclear matter or hadronic matter. It is target source particle, regarding the nuclear limiting fragmentation regime.

### Forward Emitted Pion Multiplicity Characteristics

The forward emitted shower particle multiplicity distributions of  $3.7A$  GeV  $^{16}\text{O}$  interactions with emulsion nuclei at average impact parameters are shown in Fig. (4). The interactions with H, CNO, Em, and AgBr are presented in insets a, b, c, and d, respectively.

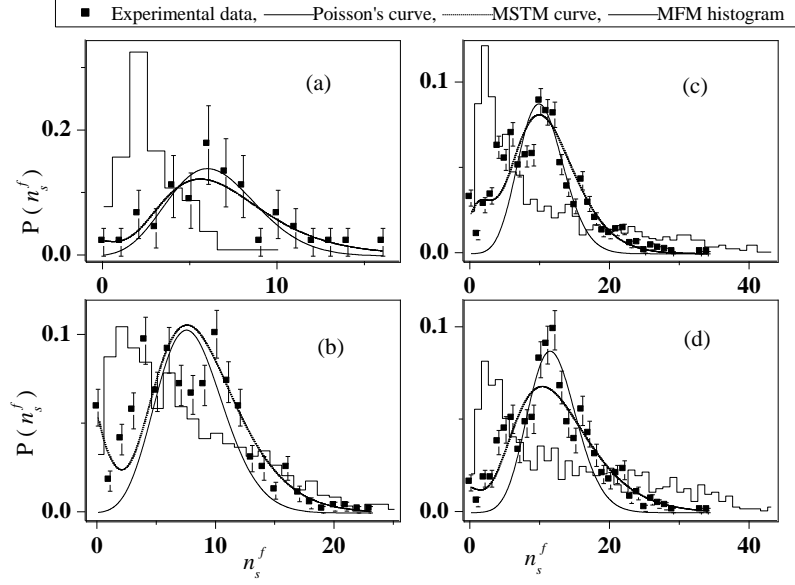


**Fig. (4): Multiplicity distributions of the forward emitted shower particle in 3.7A GeV  $^{16}\text{O}$  interactions with H, CNO, Em, and AgBr nuclei at average impact parameters.**

Unlike the observed behavior of the backward emitted shower particle, the characteristic feature, here, is the peaking curve shapes. The multiplicity range as well as the broadening of the distributions increases with target size. The geometrical model considering the overlap size between target and projectile seems to be effective in drawing the characteristic features of the distributions. Accordingly the effect of the target size is reflected on the impact parameter value and consequently on the energy participation, which is the main effective parameter in particle creation. In this concept, the average multiplicity increases with the target size as shown in Table (4). The MFM can not estimate the data. It reproduces qualitatively the distributions at higher multiplicities only in insets b, c, and d. The average multiplicities,  $\langle n_s^f \rangle_{\text{MFM}}$ , can be predicted by the MFM except for H target nuclei events. The distributions are fitted by the Poisson's law of Eq. (4).

$$P(n_s^f) = p_s^f \frac{\langle n_s^f \rangle^{n_s^f}}{n_s^f!} e^{-\langle n_s^f \rangle} \quad (4)$$

The normalization factor,  $p_s^f$ , and  $\langle n_s^f \rangle_{\text{Poisson}}$  of Eq. (4) are obtained as fit parameters. They are placed in Table (4). The average multiplicity is predicted well by Poisson's law. The dispersion of the forward emitted shower particle multiplicity is defined by Eq. (5). The experimental dispersion values,  $D_{\text{Exp}}$ , and the simulated values,  $D_{\text{MFM}}$ , are listed in Table (4). From the table the dispersion increases with the target size. The simulated values overestimate the experimental ones except for the events associated with H target nuclei.

$$D = \sqrt{\langle (n_s^f)^2 \rangle - \langle n_s^f \rangle^2} \quad (5)$$

**Table (4): Characteristic parameters associated with the forward emitted shower particle multiplicity in 3.7A GeV  $^{16}\text{O}$  interactions with emulsion nuclei at average impact parameters.**

Target		H	CNO	Em	AgBr
	$p_s^f$	0.89±0.08	0.73±0.08	0.70±0.06	0.75±0.05
	$\langle n_s^f \rangle_{\text{Poisson}}$	6.45±0.33	7.95±0.44	10.22±0.40	11.83±0.35
	$\langle n_s^f \rangle_{\text{Exp}}$	6.64±1.08	7.65±0.32	10.10±0.26	11.84±0.40
	$\langle n_s^f \rangle_{\text{MFM}}$	2.60	7.18	10.15	12.86
	$D_s^f_{\text{Exp}}$	3.39±0.55	4.43±0.19	5.60±0.16	5.70±0.19
	$D_s^f_{\text{MFM}}$	1.84	5.41	9.66	10.54
j = 1	$k_1$	0.80	0.90	0.80	0.86
	$m_1$	5	6	7	5
	$\langle n_{i1} \rangle$	1.41	1.50	1.67	2.58
j = 2	$k_2$	0.20	0.05	0.12	0.04
	$m_2$	1	2	2	2
	$\langle n_{i2} \rangle$	8.256	1.421	2.402	0.002
j = 3	$k_3$	–	0.05	0.08	0.10
	$m_3$	–	1	1	1
	$\langle n_{i3} \rangle$	–	0.93	3.41	7.28
	$\langle n_s^f \rangle_{\text{MSTM}}$	7.29	8.29	10.20	11.82

In the framework of the MSTM, the distributions are reproduced well. The obtained average multiplicities,  $\langle n_s^f \rangle_{\text{MSTM}}$ , agree perfectly with the experimental data. Table (4) data indicate that there are 3 subgroups of sources responsible for this production system. However, the 3<sup>rd</sup> subgroup has weak weight factors. In H target data 2 subgroups are found only. The 1<sup>st</sup> subgroup forms, at least, 80% of the sources. It consists of 5 to 7 sources. Hence, the forward emitted pion multiplicity distribution is a superposition of multisource characterized by the peaking shaped curve. It is reasonable to say that the mechanism of particle production in the FHS is completely different from that in the BHS.

Exactly, there is no strict definition of what is meant by central collisions. To find the physical quantities that are sensitive to the centrality at high energy, it is important to understand the behavior of the very hot and dense nuclear matter formed in the nuclear collisions. It is suggested that the forward emitted pion comes from the hadronic matter. Hence, it is convenient to define the present centrality parameter on the basis of the nuclear matter size. The nuclear matter is contributed from the target and projectile nuclei. The grey particle multiplicity,  $N_g$ , indicates the target nuclear matter size and the participant projectile proton multiplicity,  $N_p$ , indicates the projectile nuclear matter size. Hence, the centrality parameter ( C ) can be defined by Eq. (6).

$$C = N_g + N_p \quad (6)$$

Fig. (6) shows the forward emitted pion multiplicity at different centralities of 3.7A GeV  $^{16}\text{O}$  interaction with CNO emulsion nuclei. The centrality ranges,  $0 \leq C \leq 5$ ,  $C = 6$ ,  $C = 7$ ,  $8 \leq C \leq 9$ , and  $C \geq 10$  are associated with insets a, b, c, d, and e, respectively.

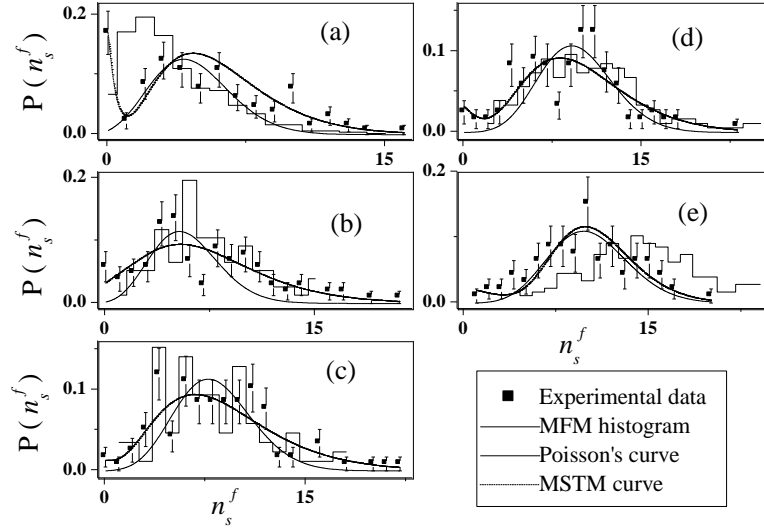


**Fig. (5): Multiplicity distributions of the forward emitted shower particle in 3.7A GeV  $^{16}\text{O}$  interactions with CNO emulsion nuclei at different centralities.**

From Fig. (5), the peaking shaped curves are a characteristic of the distributions. The multiplicity tail grows with the centrality. The peak shifts forward with the centrality. The distributions become near to be symmetric about the peak in insets c, d, and e associated with centralities,  $C > 6$ . The symmetry implies a similarity to the Gaussian shape associated with the isotropy of state. In this state, the contributions of the multi sources to the production system are equivalent. Hence at in the central region of this collision system the isotropy of state almost exists. This is confirmed by the good agreement with the MSTM observed in Fig. (5) or Table (5). The MFM can reproduce the distributions well in insets b, c, and d. The distributions can be reproduced well by the Poisson's law of Eq. (4). The corresponding fit parameters are listed in Table (5). The average multiplicities predicted from Poisson's law increase with the centrality. They are nearly the same as the experimental ones. The simulated values of the MFM are similar to the experimental ones at  $C = 6$  and  $C = 7$ . At  $C > 6$ , the simulated MFM values overestimate the data. The dispersion values fluctuate with the centrality. The simulated MFM dispersions are nearly similar to the data.

**Table (5): Characteristic parameters associated with the forward emitted shower particle multiplicity in 3.7A GeV  $^{16}\text{O}$  interactions with CNO emulsion nuclei at different centralities.**

Centrality	$0 \leq C \leq 5$	$C = 6$	$C = 7$	$8 \leq C \leq 9$	$C \geq 10$	
$p_s^f$	$67.38 \pm 14.15$	$69.88 \pm 10.43$	$82.60 \pm 0.27$	$82.26 \pm 9.10$	$86.76 \pm 7.58$	
$\langle n_s^f \rangle_{\text{Poisson}}$	$4.60 \pm 0.63$	$5.78 \pm 0.50$	$8.17 \pm 0.45$	$9.55 \pm 0.48$	$10.17 \pm 0.39$	
$\langle n_s^f \rangle_{\text{Exp}}$	$4.95 \pm 0.33$	$6.94 \pm 0.69$	$8.23 \pm 0.76$	$8.84 \pm 0.81$	$9.86 \pm 1.03$	
$\langle n_s^f \rangle_{\text{MFM}}$	3.50	7.05	7.79	10.23	14.17	
$D_s^f_{\text{Exp}}$	$3.74 \pm 0.23$	$4.24 \pm 0.42$	$4.19 \pm 0.39$	$4.19 \pm 0.38$	$3.89 \pm 0.41$	
$D_s^f_{\text{MFM}}$	2.64	3.21	3.80	4.47	4.46	
$j = 1$	$k_1$	0.93	0.60	0.90	0.52	0.90
	$m_1$	4	4	4	5	11
	$\langle n_{i1} \rangle$	1.53	2.16	2.26	1.81	0.98
$j = 2$	$k_2$	0.07	0.30	0.01	0.42	0.1
	$m_2$	1	2	2	6	1



	$\langle n_{i2} \rangle$	0.41	3.08	6.88	1.88	3.92
j = 3	$k_3$	—	0.10	0.09	0.06	—
	$m_3$	—	1	1	1	—
	$\langle n_{i3} \rangle$	—	0.36	1	1	—
$\langle n_s^f \rangle_{\text{MSTM}}$		5.72	7.07	8.37	9.51	10.09

Fig. (6) shows the forward emitted pion multiplicity at different centralities of 3.7A GeV  $^{16}\text{O}$  interaction with AgBr emulsion nuclei. The centrality ranges,  $0 \leq C \leq 6$ ,  $7 \leq C \leq 8$ ,  $9 \leq C \leq 10$ ,  $11 \leq C \leq 12$ ,  $13 \leq C \leq 14$ , and  $C \geq 15$  are associated with insets a, b, c, d, e, and f, respectively.

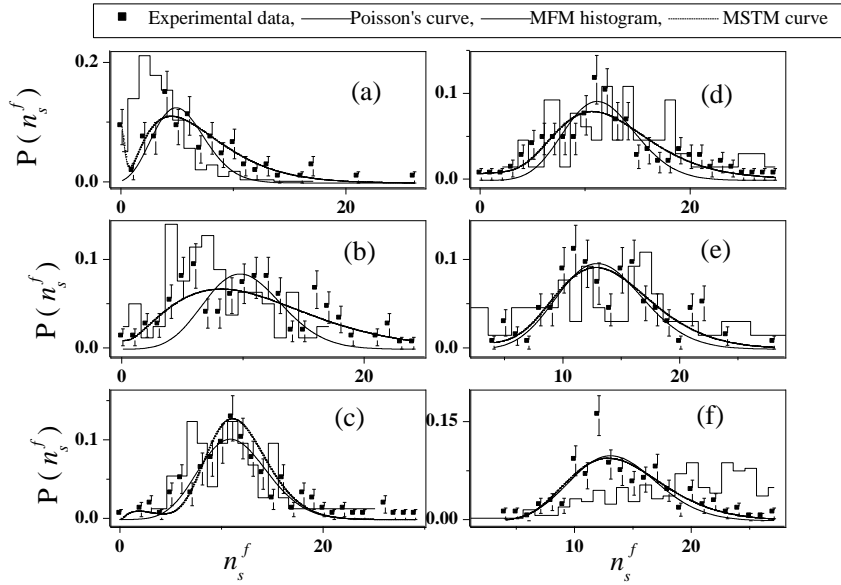


**Fig. (6): Multiplicity distributions of the forward emitted shower particle in 3.7A GeV  $^{16}\text{O}$  interactions with AgBr emulsion nuclei at different centralities.**

From Fig. (6), the peaking shaped curves are a characteristic of the distributions. The growth of the multiplicity tail stops at the onset of centrality of  $C \sim 9$ , as observed in insets c, d, e, and f. The peak shifts forward with the centrality. The distributions become near to be symmetric about the peak in insets b, c, d, e, and f where the isotropy in the multisource superposition is expected to exist. This is confirmed by the good agreement with the MSTM observed in Fig. (6) or Table (6). The MFM can reproduce the distributions well in insets b, c, d, and e. The distributions can be reproduced well by the Poisson's law of Eq. (4). The corresponding fit parameters are listed in Table (6). The average multiplicities predicted from Poisson's law increase with the centrality. They are nearly the same as the experimental ones. The simulated values of the MFM underestimate the data up to  $C = 10$  while at  $C > 10$  the overestimation is the trend. The dispersion values fluctuate with the centrality. The simulated MFM dispersions are nearly similar to the data.

**Table (6): Characteristic parameters associated with the forward emitted shower particle multiplicity in 3.7A GeV  $^{16}\text{O}$  interactions with AgBr emulsion nuclei at different centralities.**

Centrality	$0 \leq C \leq 6$	$7 \leq C \leq 8$	$9 \leq C \leq 10$	$11 \leq C \leq 12$	$13 \leq C \leq 14$	$C \geq 15$	
$p_s^f$	$0.73 \pm 0.10$	$0.68 \pm 0.10$	$0.86 \pm 0.05$	$0.78 \pm 0.06$	$0.89 \pm 0.08$	$0.92 \pm 0.08$	
$\langle n_s^f \rangle_{\text{Poisson}}$	$5.30 \pm 0.40$	$10.16 \pm 0.64$	$11.28 \pm 0.26$	$11.54 \pm 0.35$	$13.34 \pm 0.46$	$13.49 \pm 0.43$	
$\langle n_s^f \rangle_{\text{Exp}}$	$6.29 \pm 0.61$	$10.36 \pm 0.85$	$11.99 \pm 0.96$	$12.30 \pm 1.02$	$13.83 \pm 1.19$	$14.22 \pm 1.08$	
$\langle n_s^f \rangle_{\text{MFM}}$	3.45	7.41	10.56	12.89	14.44	18.72	
$D_s^f_{\text{Exp}}$	$4.65 \pm 0.45$	$5.38 \pm 0.44$	$5.29 \pm 0.43$	$5.62 \pm 0.47$	$4.59 \pm 0.40$	$4.58 \pm 0.35$	
$D_s^f_{\text{MFM}}$	2.45	3.93	3.98	5.52	6.12	5.71	
j = 1	$k_1$	0.63	0.83	0.95	0.80	0.90	0.97
	$m_1$	4	4	15	7	11	11
	$\langle n_{i1} \rangle$	2.06	3.12	0.78	1.78	1.28	1.27
j = 2	$k_2$	0.35	0.14	0.05	0.15	0.10	0.03
	$m_2$	3	3	2	2	2	1
	$\langle n_{i2} \rangle$	1.46	1.86	1.70	8.07	5.46	27.27
j = 3	$k_3$	0.02	0.03	–	0.05	–	–
	$m_3$	1	1	–	1	–	–
	$\langle n_{i3} \rangle$	0.21	3.16	–	6.30	–	–
$\langle n_s^f \rangle_{\text{MSTM}}$	6.72	11.23	11.29	12.71	13.76	14.37	

## CONCLUSIONS

From the analysis of 3.7A GeV  $^{16}\text{O}$  interaction, using photographic nuclear emulsion detector, we conclude the following:

1- The inelastic interaction cross section of  $^{16}\text{O}$  in nuclear emulsion is approximated by a power law relation as a function of the target mass number independent on the energy. It agrees with the predictions of the Glauber's approach.

2- The dominant mechanism characterizing the backward emitted pion production is the decay behavior. The multiplicity distribution of this pion is determined in terms of the target size. The energy or projectile size is not effective in this production system. The backward emitted pion multiplicity characteristics depend on the target size, regarding the nuclear limiting fragmentation beyond  $E_{\text{lab}} \sim 1$  to 2A GeV. Thus, such pion is expected to be decayed through the de-excitation of the excited target nucleus as similar as the compound nucleus mechanism. The MFM qualitatively agrees with the backward emitted pion multiplicity characteristics. The MSTM implies that this production system is a single source indicated by the decay curve.

3- In the FHS the pion multiplicity distributions are peaking shaped, where they can be approximated by the Poisson's law. The production of the forward emitted pion is attributed to a mechanism, which is completely different from that in BHS. Although the target nucleus is not the source of this pion, however the target size is an effective parameter in this production as well as the projectile size. The effect of the target size is reflected on their multiplicity characteristics at each target. Regarding the incident energy role as a principal parameter affecting the forward relativistic hadron production, this production is creation system. The particles are sourced from hadronic matter or fireball nuclear matter. The MSTM implies that this system is multisource superposition. In  $^{16}\text{O}+\text{CNO}$  and  $^{16}\text{O}+\text{AgBr}$  collisions the isotropy of state is suggested to exist at  $C > 6$ . The MFM can not estimate the data at average impact parameter or in peripheral regions. At higher centralities the MFM reproduces the distributions.

## ACKNOWLEDGEMENT

We owe much to Vekseler and Baldin High Energy Laboratory, JINR, Dubna, Russia, for supplying us the photographic emulsion plates irradiated at Synchrophasotron.

## REFERENCES

- 1 Benecke J, Chou T T, Yang C N, Yen E. Phys. Rev.,1969, **188**, 2159.
- 2 Fu–Hu Liu. Chinese Journal of Physics,2002, **40**, 159.
- 3 Ahmad M S, Khan M Q R, Hasan R. Nucl. Phys. A,1989, **499**, 821.
- 4 Webber W R. Proceedings of the international Cosmic Ray Conference, Vol. 8, P. 65, Moscow, USSR (1987).
- 5 Lindstorm P L, Greiner D E, Heckman H H, Cork B. Lawrence Berkeley Laboratory Report, LBL–3650, 1975.
- 6 Olson D L, Berman B L, Grenier D E, Heckman H H, Lindstrom P J, Crawford H J. Phys. Rev. C, 1983, **28**, 1602.
- 7 El–Nagdy M S, Abdelsalam A, Abou–Moussa Z, Badawy B M. Can. J. Phys.,2013, **91**, 737.
- 8 Shmakov S Yu, Uzhinskii V V. Com. Phys. Comm.,1989, **54**, 125.
- 9 Andersson B, Gustafson G, Nilsson–Almqvist B. Nucl. Phys. B,1987, **281**, 289.
- 10 Nilsson–Almqvist B, Stenlund E. Comp. Phys. Comm.,1987, **43**, 387.
- 11 Fu–Hu Liu Nucl. Phys. A, 2008, **810**, 159.
- 12 Fu-Hu Liu, Qi-Wen Lu, Bao-Chun Li, Bekmirzaev R. Chinese Journal of Physics 2011, **49**, 601.
- 13 Rahim M A, Fakhraddin S, Asharabi H. Eur. Phys. J. A, 2012, **48**, 115.
- 14 Abdelsalam A, Metwalli N, Kamel S, Aboullela M, Badawy B M, Abdallah N. Can. J. Phys.,2013, **91**, 438.
- 15 Abdelsalam A, Badawy B M, Hafiz M. J. Phys. G: Nucl. Part. Phys.,2012, **39**, 105104.
- 16 Powell C F, Fowler F H, Perkins D H. The Study of Elementary Particles by the Photographic Method, Pergamon Press. London; New York, Paris, Los Angeles, 474 (1958).
- 17 Barkas H. Nuclear Research Emulsion, Vol. I, Technique and Theory Academic Press Inc., (1963).
- 18 Abdelsalam A., El–Nagdy M S, Badawy B M, Osman W, Fayed M. Int. J. Mod. Phys. E, 2016, **25**, 1650034.
- 19 EMU01 Collaboration, Lund University Report, Sweden, LUIP 8904, May (1989).
- 20 Abdelsalam A, El–Nagdy M S, Badawy B M; Can. J. Phys.,2011, **89**, 261.